



Porphyrins Ia,b were treated as synthetic intermediates in the present study, so their purification was not pursued.

**5-[2-[(2,2,6,6-Tetramethyl-4-piperidinyl-1-oxy)amido]phenyl]-10,15,20-tritylporphyrin (II).** The amide was prepared from the acid chloride of 5-(2-carboxyphenyl)-10,15,20-tritylporphyrin<sup>4,11</sup> and 4-amino-2,2,6,6-tetramethylpiperidinyl-1-oxy by the procedure described for Ia. The product was recrystallized from CH<sub>2</sub>Cl<sub>2</sub>/hexane: yield 83%; IR  $\nu_{\text{NH}}$  3540, 3420 cm<sup>-1</sup>,  $\nu_{\text{CO}}$  1650 cm<sup>-1</sup>; Vis 644 (3.75), 593 (3.80), 554 (3.97), 518 (4.28), 421 (5.69); EPR  $g = 2.0059$ ,  $A_N = 16.0$  G. Anal. Calcd for C<sub>57</sub>H<sub>53</sub>N<sub>6</sub>O<sub>2</sub>: C, 80.16; H, 6.25; N, 9.84. Found: C, 80.29; H, 6.21; N, 9.71.

**Preparation of Vanadyl Porphyrins.** The long reflux times required to prepare the vanadyl complexes in DMF solution resulted in cleavage of the amide linkages in Ia,b and II. Therefore it was necessary to prepare the vanadyl complexes by a different route. The vanadyl complex of the cis isomer (IIIb) was made by first preparing the *cis*-acrylic acid complex. However, the trans isomer of the acrylic acid porphyrin is less thermally stable than is the cis isomer, so the vanadyl complex was first made by using the *trans*-acrylic acid ester, which was then hydrolyzed to the acid form and condensed with the nitroxyl.

**Vanadyl *meso*-Tetraphenylporphyrin-1-*trans*-acrylic Acid Ethyl Ester (VIIIa).** *meso*-Tetraphenylporphyrin-1-*trans*-acrylic acid ethyl ester<sup>3,10</sup> (0.70 g, 1.0 × 10<sup>-3</sup> mol) was dissolved in 150 mL of DMF. VOSO<sub>4</sub> (0.82 g, 5 × 10<sup>-3</sup> mol) was added and the mixture was heated at about 100 °C for 100 h. The mixture was cooled and poured into 200 mL of H<sub>2</sub>O. The precipitate was collected by filtration, dried, and chromatographed on silica gel in CHCl<sub>3</sub> solution. The product was recrystallized from CH<sub>2</sub>Cl<sub>2</sub>/hexane: yield 67%; IR  $\nu_{\text{CO}}$  1710 cm<sup>-1</sup>,  $\nu_{\text{C=C}}$  1590 cm<sup>-1</sup>; Vis 594 (3.78), 556 (4.19), 434 (5.36); EPR (CHCl<sub>3</sub>)  $g = 1.9801$ ,  $A_V = 94.0$  G. Anal. Calcd for C<sub>47</sub>H<sub>32</sub>N<sub>4</sub>O<sub>5</sub>V: C, 75.10; H, 4.29; N, 7.45. Found: C, 75.38; H, 4.58; N, 7.15.

**Vanadyl *meso*-Tetraphenylporphyrin-1-*trans*-acrylic Acid (IXa).** Ethyl ester VIIIa (0.378 g, 5.0 × 10<sup>-4</sup> mol) was dissolved in 50 mL of pyridine. Twenty milliliters of 2 N KOH in MeOH was added and the solution was stirred for 24 h at room temperature. The extent of reaction was checked by TLC on silica gel with CHCl<sub>3</sub> as eluant. The solvent was removed under vacuum and the residue was neutralized with 2 N HCl. The product was extracted into CHCl<sub>3</sub> and dried over Na<sub>2</sub>SO<sub>4</sub>. The volume of the CHCl<sub>3</sub> solution was reduced to 20 mL and the solution was put on a silica gel column. A small amount of unreacted ester eluted first. The acid was eluted with CHCl<sub>3</sub> containing 2% ethanol and recrystallized from CHCl<sub>3</sub>/heptane: yield 80%; IR  $\nu_{\text{OH}}$  3500 cm<sup>-1</sup>,  $\nu_{\text{CO}}$  1690 cm<sup>-1</sup>,  $\nu_{\text{C=C}}$  1600 cm<sup>-1</sup>; Vis 594 (3.97), 555 (4.38), 435 (5.55); EPR  $g = 1.9801$ ,  $A_V = 94.5$  G.

**Vanadyl *meso*-Tetraphenylporphyrin-1-*cis*-acrylic Acid (IXb).** *meso*-Tetraphenylporphyrin-1-*cis*-acrylic acid<sup>3,10</sup> (0.66 g, 1.0 × 10<sup>-3</sup> mol) was dissolved in 150 mL of DMF. VOSO<sub>4</sub> (0.815 g, 5.0 × 10<sup>-3</sup> mol) was added and the mixture was refluxed for 24 h. The reaction mixture was cooled and poured into 200 mL of H<sub>2</sub>O. The precipitate was collected and dried under vacuum. The crude product was chromatographed on silica gel in CHCl<sub>3</sub>. The product was eluted with CHCl<sub>3</sub> containing 2% ethanol and recrystallized from CHCl<sub>3</sub>/heptane: yield 69%. The acid is not stable to prolonged heating. IR  $\nu_{\text{OH}}$  3500 cm<sup>-1</sup>,  $\nu_{\text{CO}}$  1700 cm<sup>-1</sup>,  $\nu_{\text{C=C}}$  1590 cm<sup>-1</sup>; Vis 591 (3.55), 552 (4.18), 430 (5.37); EPR (CHCl<sub>3</sub>)  $g = 1.9801$ ,  $A_V = 94.5$  G.

**Vanadyl *meso*-Tetraphenylporphyrin-1-[3-[N-(2,2,6,6-tetramethylpiperidinyl-1-oxy)acrylamido]porphyrin (IIIa,b).** The amides were prepared from the acid chlorides of IXa or IXb and 4-amino-2,2,6,6-tetramethylpiperidinyl-1-oxy by the procedure described for Ia.

**Trans Isomer (IIIa).** The product was recrystallized from CH<sub>2</sub>Cl<sub>2</sub>/hexane: yield 56%; IR  $\nu_{\text{NH}}$  3450 cm<sup>-1</sup>,  $\nu_{\text{CO}}$  1645 cm<sup>-1</sup>,  $\nu_{\text{C=C}}$  1590 cm<sup>-1</sup>; Vis 593 (3.82), 554 (4.26), 435 (5.44). Anal. Calcd for C<sub>56</sub>H<sub>47</sub>N<sub>6</sub>O<sub>3</sub>V: C, 74.49; H, 5.25; N, 9.31. Found: C, 74.08; H, 5.17; N, 9.46. The low carbon analysis is consistent with the presence of about 5 mol % of the amino nitroxyl, which is difficult to separate from the product by chromatography. Since the line widths of the nitroxyl signals in the vanadyl complex are only slightly broader than for the amino nitroxyl and the  $g$  values are the same, a small amount of nitroxyl would not be detectable in the EPR spectrum.

**Cis Isomer (IIIb).** The product was recrystallized from CH<sub>2</sub>Cl<sub>2</sub>/hexane: yield 47%; IR  $\nu_{\text{NH}}$  3500 cm<sup>-1</sup>,  $\nu_{\text{CO}}$  1650 cm<sup>-1</sup>,  $\nu_{\text{C=C}}$  1590 cm<sup>-1</sup>; Vis 591 (3.67), 552 (4.20), 430 (5.38). Anal. Calcd for C<sub>56</sub>H<sub>47</sub>N<sub>6</sub>O<sub>3</sub>V: C, 74.49; H, 5.25; N, 9.31. Found: C, 74.26; H, 5.11; N, 9.11.

**Preparation of Silver(II) Porphyrins.** Silver(II) *meso*-Tetraphenylporphyrin-1-[3-[N-(2,2,6,6-tetramethylpiperidinyl-1-oxy)acrylamido]porphyrin (IVa,b). Ia or Ib (0.084 g, 1.0 × 10<sup>-4</sup> mol) was dissolved in 100 mL of acetonitrile. Silver acetate (0.020 g, 1.2 × 10<sup>-4</sup> mol) was added and the

mixture was refluxed for 20 min. The solvent was removed under vacuum and the residue was dissolved in CHCl<sub>3</sub>. The CHCl<sub>3</sub> solution was washed three times with H<sub>2</sub>O and dried over Na<sub>2</sub>SO<sub>4</sub>. After the solution was reduced to 15 mL the CHCl<sub>3</sub> solution was put on a silica gel column. Elution with CHCl<sub>3</sub> gave a rapidly moving red band which contained the product.

**Trans Isomer (IVa).** The product was recrystallized from CH<sub>2</sub>Cl<sub>2</sub>/hexane: yield 80%; IR  $\nu_{\text{NH}}$  3400 cm<sup>-1</sup>,  $\nu_{\text{CO}}$  1650 cm<sup>-1</sup>,  $\nu_{\text{C=C}}$  1590 cm<sup>-1</sup>; Vis 581 (3.90), 549 (4.30), 435 (5.49). Anal. Calcd for C<sub>56</sub>H<sub>47</sub>AgN<sub>6</sub>O<sub>2</sub>: C, 71.26; H, 5.02; N, 8.90. Found: C, 71.33; H, 5.15; N, 8.81.

**Cis Isomer (IVb).** The product was recrystallized from CH<sub>2</sub>Cl<sub>2</sub>/hexane: yield 76%; IR  $\nu_{\text{NH}}$  3400 cm<sup>-1</sup>,  $\nu_{\text{CO}}$  1640 cm<sup>-1</sup>,  $\nu_{\text{C=C}}$  1590 cm<sup>-1</sup>; Vis 578 (3.33), 543 (4.27), 430 (5.56). Anal. Calcd for C<sub>56</sub>H<sub>47</sub>AgN<sub>6</sub>O<sub>2</sub>: C, 71.26; H, 5.02; N, 8.90. Found: C, 71.35; H, 5.01; N, 8.78.

**Silver(II) 5-[2-[(2,2,6,6-Tetramethylpiperidinyl-1-oxy)amido]phenyl]-10,15,20-tritylporphyrin (V).** The complex was prepared from II and silver acetate, using the procedure described for IVa,b, and recrystallized from CH<sub>2</sub>Cl<sub>2</sub>/hexane: yield 83%; IR  $\nu_{\text{NH}}$  3540 cm<sup>-1</sup>,  $\nu_{\text{CO}}$  1660 cm<sup>-1</sup>; Vis 575 (3.79), 543 (4.28), 428 (5.64). Anal. Calcd for C<sub>57</sub>H<sub>51</sub>AgN<sub>6</sub>O<sub>2</sub>: C, 71.32; H, 5.36; N, 8.76. Found: C, 71.23; H, 5.17; N, 8.56.

**Computer Simulations.** The EPR spectra were simulated by using the computer program CUNO.<sup>9</sup> The Hamiltonian used was

$$\mathcal{H} = g_1 \beta H \hat{S}_{1z} + g_2 \beta H \hat{S}_{2z} + h J \hat{S}_{1z} \hat{S}_{2z} + \frac{hJ}{2} (\hat{S}_{1+} \hat{S}_{2-} + \hat{S}_{1-} \hat{S}_{2+}) + h A_M \hat{S}_{1z} \hat{I}_{1z} + h A_N \hat{S}_{1z} \hat{I}_{2z} + h A_N \hat{S}_{2z} \hat{I}_{3z} + \frac{h A_M}{2} (\hat{S}_{1+} \hat{I}_{1-} + \hat{S}_{1-} \hat{I}_{1+}) - g_M \beta M H \hat{I}_{1z} - g_N \beta N H \hat{I}_{2z} - g_N \beta N H \hat{I}_{3z} \quad (1)$$

where  $g_1$  and  $g_2$  are the  $g$  values of the metal and nitroxyl electrons,  $\hat{S}_1$  and  $\hat{S}_2$  refer to the metal and nitroxyl electron spins, respectively,  $J$  is the electron-electron coupling constant in hertz,  $I_1$ ,  $I_2$ , and  $I_3$  refer to the metal electron spin, the nuclear spin of the coordinated nitrogens, and the nuclear spin of the nitroxyl nitrogen, respectively,  $A_M$  is the metal electron-metal nucleus coupling constant in hertz,  $A_N$  is the coupling constant in hertz between the metal electron and the nuclear spins of the coordinated nitrogens,  $A_N'$  is the coupling constant in hertz between the nitroxyl electron and nuclear spin of the nitroxyl nitrogen, and all other symbols are defined as in ref 9. The first seven terms in the Hamiltonian were treated exactly and the last four were treated as a perturbation to second order for the transition energies and to first order for the transition probabilities. To facilitate visual comparison with the field-swept experimental spectra the values of  $J$ ,  $A_M$ ,  $A_N$ , and  $A_N'$  are discussed below in units of gauss with the conversion between hertz and gauss given by eq 2-4. The conversion factor for  $A_N$  is the same as for  $A_M$ . Only the absolute value of  $J$  can be determined from these experiments.

$$J \text{ (G)} = J \text{ (Hz)} \cdot \frac{h}{2\beta} \left( \frac{1}{g_1} + \frac{1}{g_2} \right) \quad (2)$$

$$A_M \text{ (G)} = A_M \text{ (Hz)} \cdot \frac{h}{g_1 \beta} \quad (3)$$

$$A_N' \text{ (G)} = A_N' \text{ (Hz)} \cdot \frac{h}{g_2 \beta} \quad (4)$$

The parameters for silver(II) tetraphenylporphyrin in CHCl<sub>3</sub> solution ( $g = 2.0569$ ,  $A_{Ag} = 41.5$  G,  $A_N = 22.5$  G) were used as starting parameters in the simulation of the spectra of IVa,b and V. Contributions from <sup>107</sup>Ag and <sup>109</sup>Ag were not resolved so the hyperfine splitting constant is an average for the two isotopes. The unresolved differences were taken into account with a Gaussian contribution to the silver line shape. The spectra were interpreted as arising from spin-spin interaction between the silver and nitroxyl unpaired electrons with a coupling constant  $J$ . When  $J$  is small the nitroxyl region of the spectrum is a doublet of triplets. As  $J$  increases the outer lines of the AB pattern decrease in intensity and the inner silver and nitroxyl lines occur at an averaged position. The transitions are labeled according to the nature of the transition as  $J \rightarrow 0$ .

## Results and Discussion

The silver and vanadyl complexes of the cis and trans isomers of the spin-labeled porphyrins Ia,b have been prepared. For the free porphyrins and their silver and vanadyl complexes the transitions in the visible spectra occur at lower energy for the trans isomers than for the cis isomers, which indicates greater electronic interaction between the porphyrin ring and the vinyl group in the trans isomer than in the cis isomer.<sup>3</sup>

**EPR Spectra of Vanadyl Complexes.** The EPR spectra of the spin-labeled vanadyl complexes IIIa,b in CHCl<sub>3</sub> and pyridine

(11) Anton, J. A.; Kwong, J.; Loach, P. A. *J. Heterocycl. Chem.* **1976**, *13*, 717-25.

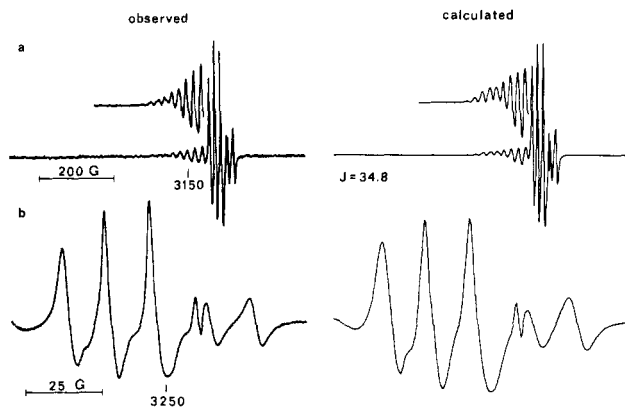


**Figure 1.** X-Band EPR spectra of the spin-labeled silver complex IVa in  $\text{CHCl}_3$  solution at room temperature: (a) 800-G scan, 125 G/min scan rate, 0.5-G modulation amplitude, 0.5 mW; (b) 100-G scan of the nitroxyl region, 12.5 G/min scan rate, 0.5-G modulation amplitude, 0.5 mW.  $J$  is given in gauss ( $1 \text{ G} \approx 10^{-4} \text{ cm}^{-1}$ ).

**Table I.** Spin-Spin Coupling Constants in Spin-Labeled Silver(II) Porphyrins

compound	solvent	$J,^a \text{ G}$	$10^4 J, \text{ cm}^{-1}$
IVa	$\text{CHCl}_3$	34.8	32.9
IVa	pyridine	46.0	43.5
IVb	toluene	$\sim 10^b$	$\sim 9.5$
IVb	$\text{CHCl}_3$	$\sim 20^b$	$\sim 19$
IVb	9:1 toluene-THF	6.5	6.2
IVb	pyridine	5.8	5.5
V	$\text{CHCl}_3$	1000 <sup>c</sup>	947
V	pyridine	125 <sup>c</sup>	118

<sup>a</sup> Based on X-band spectra unless otherwise noted. <sup>b</sup> Obtained from simulation of broad nitroxyl lines at X-band and Q-band.

<sup>c</sup> Obtained from simulation of full spectrum at X-band and Q-band.

solutions are superpositions of the typical eight-line pattern expected for the vanadyl ion and the sharp three-line pattern characteristic of a nitroxyl radical. The line widths of the nitroxyl signals in IIIa,b are about 0.3 G broader than in the spin-labeled porphyrins Ia,b. Thus the value of the spin-spin coupling constant  $J$  must be  $\leq 0.3 \text{ G}$ .

**EPR Spectra of Silver(II) Complexes.** The nitroxyl region of the EPR spectra for the trans isomer of the spin-labeled silver complex IVa in  $\text{CHCl}_3$  solution is a doublet of triplets (Figure 1) with  $J$ , the electron-electron coupling constant, equal to 34.8 G (Table I). The silver lines are partially obscured by overlap with the sharper nitroxyl lines. The computer-simulated spectrum in Figure 1 includes nitroxyl which is not interacting with silver (free nitroxyl) with a concentration 2.5% of that for IVa. This may be due to an impurity or decomposition. The elemental analysis of IVa would not be sensitive to this amount of impurity. In pyridine solution a similar spectrum was obtained with  $J = 46.0 \text{ G}$ .

The nitroxyl lines in the EPR spectra of the cis isomer IVb in toluene and  $\text{CHCl}_3$  solutions are much broader than the lines in the spectra of the trans isomer IVa. The broadness of the lines and extensive overlap of the silver and nitroxyl lines makes the interpretation of the X-band spectra rather ambiguous. However, the Q-band spectra of IVb in toluene solution (Figure 2a) show clearly separated signals for the silver and nitroxyl electrons which are consistent with  $J \sim 10 \text{ G}$ . Similar Q-band spectra were obtained in  $\text{CHCl}_3$  solution. The X-band spectra of IVb are consistent with the values of  $J$  obtained at Q-band. In the presence of coordinating solvents, the line widths for the nitroxyl lines are decreased and a doublet of triplets is observed with  $J = 6.5 \text{ G}$  in 9:1 toluene-THF solution and 5.8 G in pyridine solution (Figure 3). In the analogous spin-labeled copper complex VIb the line widths for the nitroxyl signals were also much smaller in coordinating solvents than in noncoordinating solvents.<sup>3</sup> This may be due to a weak interaction between the amide carbonyl oxygen and

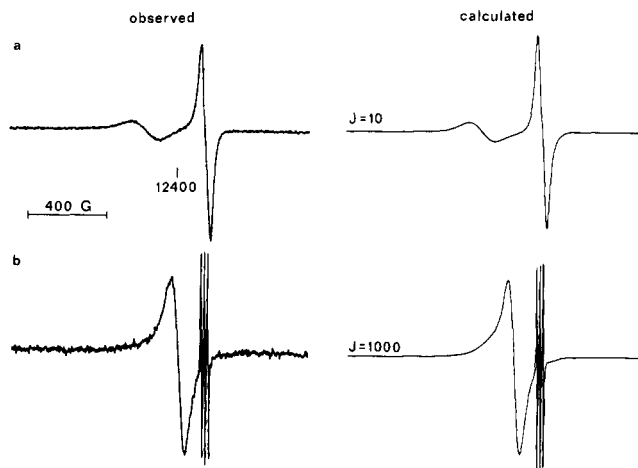


**Figure 2.** Q-Band EPR spectra at room temperature: (a) spin-labeled silver complex IVb in toluene solution, 1500-G scan, 250 G/min scan rate, 2-G modulation amplitude, 1.5 mW; (b) spin-labeled silver complex V in  $\text{CHCl}_3$  solution, 1500-G scan, 250 G/min scan rate, 2-G modulation amplitude, 47 mW. Free nitroxyl with a concentration 1.7% that of V is included in the simulation. Values of  $J$  are given in gauss.

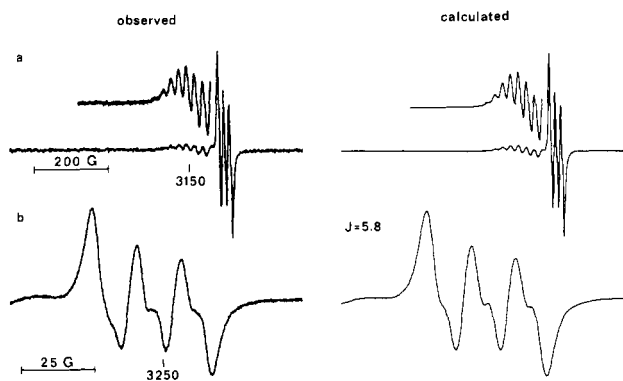


**Figure 3.** X-Band EPR spectra of the spin-labeled silver complex IVb in pyridine solution at room temperature: (a) 800-G scan, 125 G/min scan rate, 1-G modulation amplitude, 5 mW; (b) 100-G scan of the nitroxyl region, 12.5 G/min scan rate, 1-G modulation amplitude, 5 mW.  $J$  is given in gauss.

the metal ion in the absence of coordinating solvents which would provide a shorter pathway for metal-nitroxyl interaction than through the vinyl group.<sup>3</sup> Rapid fluctuations in the magnitude of this interaction could result in uncertainty in the value of  $J$  and broadening of the nitroxyl lines. Coordination of a solvent molecule as the fifth ligand on the metal could decrease the metal-nitroxyl interaction via the carbonyl oxygen.

The X-band and Q-band (Figure 2b) EPR spectra of the spin-labeled silver complex V in  $\text{CHCl}_3$  solution could both be simulated with  $J \sim 1000 \text{ G}$ . The outer lines of the AB pattern were not observed at either X-band or Q-band, but the extent of averaging of the silver and nitroxyl inner lines, which is almost complete even at Q-band, is adequate to establish the value of  $J$  with reasonable certainty. In pyridine solution the value of  $J$  is reduced to about 125 G. The large decrease in  $J$  in the presence of pyridine is similar to that observed in the analogous copper complex, VII.<sup>4</sup> In V, as in the cis isomer IVb, the carbonyl oxygen of the amide is close to the metal ion. Weak metal-oxygen interaction could provide a more direct pathway for metal-nitroxyl interaction than via the phenyl ring. This interaction could be decreased by pyridine coordination.<sup>4</sup>

**Pathway for Exchange Interactions.** It is axiomatic that exchange interactions involve overlap of orbitals and are a measure of the separation between the energy levels in the singlet and triplet manifolds. In the localized molecular orbital picture commonly used to describe chemical phenomena we may ask what is the "pathway", or sequence of atomic orbital overlaps, for the in-

teraction. In the trans vinyl complexes IIIa, IVa, and VIa it is reasonable to think in terms of overlap of metal orbitals with porphyrin orbitals providing a direct pathway to the point of attachment of the vinyl group to the porphyrin and on through the vinyl group to the nitroxyl ring. As discussed below, the larger values of  $J$  for the trans isomer than for the cis isomer in coordinating solvents indicate that the extent of delocalization through the olefin  $\pi$  orbitals correlates with the magnitude of  $J$ . The ENDOR results for CuTPP and AgTPP indicated that the metal-porphyrin interaction is a combination of  $\sigma$  and  $\pi$  effects. Similarly, the copper-nitroxyl interaction is likely due to a mix of  $\sigma$  and  $\pi$  effects. For the copper complex of the cis vinyl porphyrin IVb in noncoordinating solvents a shorter pathway for copper-nitroxyl interaction via weak interaction of the amide carbonyl oxygen with the copper was proposed.<sup>3</sup> The behavior of the silver complex IVb is similar. In the following paragraphs we examine evidence that in the phenyl-substituted complexes V and VII interaction through the porphyrin and phenyl rings may also be supplemented by a shorter pathway. The geometry of the molecules prevents intramolecular metal-nitroxyl collisions and the concentration independence of the spectra indicates that intermolecular collisions do not contribute significantly to the line shapes for  $\sim 10^{-3}$  M concentrations.

For the complexes of the trans porphyrin Ia in  $\text{CHCl}_3$  solution the value of  $J$  increases in the order  $\text{VO}^{2+}$  ( $\leq 0.3$  G)  $<$   $\text{Cu}^{2+}$  (20.0 G)  $<$   $\text{Ag}^{2+}$  (34.8 G). A similar pattern is observed in pyridine solution. For the complexes of Ib in pyridine solution  $J$  increases in the order  $\text{VO}^{2+}$  ( $\leq 0.3$  G)  $<$   $\text{Cu}^{2+}$  (3.5 G)  $<$   $\text{Ag}^{2+}$  (5.8 G) and for the complexes of IV in  $\text{CHCl}_3$  solution  $J$  increases in the order  $\text{Cu}^{2+}$  (800 G)  $<$   $\text{Ag}^{2+}$  (1000 G).

Brown and Hoffman examined the ENDOR spectra of CuTPP and AgTPP.<sup>8</sup> They found that the electron spin density on the pyrrole protons for AgTPP was 1.6 times greater than in CuTPP.<sup>5</sup> The values of  $J$  for the silver complexes of Ia,b in coordinating solvents are 1.7 times those for the analogous copper complexes in the same solvents. Thus the differences in the values of  $J$  for the silver and copper complexes parallel the spin densities at the pyrrole position. The magnitude of the nitrogen hyperfine splitting,  $A_N$ , in the EPR spectra of MTPP is also an indication of the extent of delocalization of the metal unpaired electron.<sup>4,5</sup> Values of  $A_N$  for MTPP increase in the order  $\text{VO}^{2+}$  ( $\sim 2-3$  G)  $<$   $\text{Cu}^{2+}$  (16 G)  $<$   $\text{Ag}^{2+}$  (22 G).<sup>4,5</sup> The small values of  $J$  and  $A_N$  observed for the vanadyl porphyrins imply less delocalization than for the copper and silver porphyrins. Thus the comparison with both the EPR and ENDOR data indicates that the magnitude of  $J$  for the metalloporphyrins spin-labeled on the pyrrole ring depends on the extent of delocalization of the metal unpaired electron as expected for an exchange interaction.

For the copper and silver complexes the value of  $J$  is greater for the trans porphyrin Ia than for the cis porphyrin Ib in coordinating solvents. The electronic spectra indicate that conjugation

of the porphyrin and vinyl groups is greater for the trans isomer than for the cis isomer.<sup>2</sup> Thus  $J$  is larger when there is more extensive electronic interaction as expected for an exchange interaction.

The larger value of  $J$  for the complexes of II in noncoordinating solvents than for complexes of Ia and the strong solvent dependence of  $J$  in the complexes of II can be rationalized in terms of spin densities and multiple pathways for the exchange interaction. Spin densities, as indicated by ENDOR studies of CuTPP and AgTPP, are less on the ortho protons of the phenyl rings than on the pyrrole protons.<sup>8</sup> Thus the model of exchange interaction via orbital overlap would predict that a nitroxyl attached via an amide linkage would yield a smaller  $J$  when placed at the ortho phenyl position than at the pyrrole position. The intervening vinyl group in the complexes of Ia would not greatly affect this conclusion since  $J$  for the copper complex VIa is about one-third the size of  $J$  for a porphyrin with the amide group substituted directly on the pyrrole.<sup>5</sup> In the context of this model it is surprising that  $J$  is much larger for complexes of II than for complexes of Ia. For example, in  $\text{CHCl}_3$  solution  $J$  for V, the  $\text{Ag}^{2+}$  complex of II, is about 1000 G while  $J$  for IVa, the  $\text{Ag}^{2+}$  complex of Ia, is 34.8 G. As discussed above for the comparison of the cis and trans vinyl complexes, the greater metal-nitroxyl interaction in the ortho-substituted complexes than predicted by spin density results is speculated to be due to an alternate, more direct, pathway for metal-nitroxyl interaction. Weak orbital overlap between the metal and the amide oxygen in the ortho-substituted complex would provide such a pathway. Since competition with solvent coordination would be expected to decrease the importance of this interaction pathway, the observation of smaller values of  $J$  for V and VII in coordinating solvents than in noncoordinating solvents supports this interpretation.

There are several other reports in the literature of EPR spectra which are consistent with strong exchange interaction between nitroxyl radicals and vanadyl or manganese ions.<sup>12-14</sup> The spectra reported in this paper are the first examples for a metal other than  $\text{Cu}^{2+}$  in which the full AB patterns have been observed. This observation and the trends in  $J$  as a function of metal ion and ligand structure demonstrate a greater generality for the concepts of metal-nitroxyl exchange interactions than was supported by previous reports.

**Acknowledgment.** This work was supported in part by the National Institutes of Health (Grant GM 21156). The Q-band accessory was funded in part by the National Science Foundation (Grant CHE 78-16195). Elemental analyses were performed by Spang Microanalytical Laboratory.

(12) Richardson, P. F.; Kreilick, R. W. *Chem. Phys. Lett.* **1977**, *50*, 333-5.

(13) Richardson, P. F.; Kreilick, R. W. *J. Magn. Reson.* **1978**, *29*, 285-91.

(14) Richardson, P. F.; Kreilick, R. W. *J. Phys. Chem.* **1978**, *82*, 1149-51.